Supplementary Information for

Early detection of lithium battery leakageusing a highly sensitive in situ ZIF-8membrane-coated micro-nano optical fibre

Shunfeng Sheng[1†], Hao Li[1†], Yi Zhang[2], Liangye Li[1], Kai Xiao[1], Xiukang Huang[1], Yunfei Liu[1], Wangyang Xu[1], Zhen Li[2], Lisong Yan[1], Zhijun Yan[1], Yunhui Huang[2], Qizhen Sun[1,*]

[1] *School of Optical and Electronic Information, Huazhong University of Science and Technology, Wuhan, Hubei, 430074, China.*

[2] *State Key Laboratory of Material Processing and Die & Mould Technology, School of Materials Science and Engineering, Huazhong University of Science and Technology, Wuhan, Hubei, 430074, China.*

** Corresponding author*

Email: qzsun@mail.hust.edu.cn

Details about the transmission spectrum of MNFs after four growth cycles modification (Fig. S1); The SEM image of purified ZIF-8 powder (Fig. S2a); The thickness of ZIF-8 membrane on MNFs in SEM image (Fig. S2b); The X-Ray diffraction of ZIF-8membarane on MNFs (Fig. S2c); The test of 15 cycles reused times (Fig. S3a); The Bland-Altman error analysis of 15 reused cycles (Fig. S3b). The table of VOCs sensor performance in last decade (Table. S1).

Contents

Section 1. The transmission spectrum of MNFs*ZIF

The transmission spectrum of MNFs before and after four growth cycles modification is exhibited in Fig. S1, indicating the effective modification of MNFs by ZIF-8 membrane. The four growth cycles ZIF-8 membrane increase the external refractive index, making the FSR of interference spectrum increase. It is worth noting that the transmitted optical power after the modification should theoretically decrease, but due to the optical losses in SMF patch cords is different when each time connected to wavelength demodulator, it instead shows an increase.

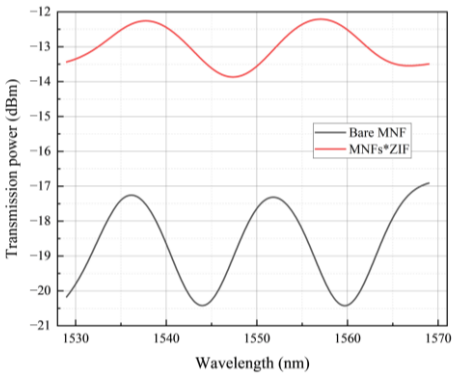

Fig. S1. The transmission spectrum of MNFs before and after 4 cycles in situ self-assembled ZIF-8 membrane functionalize.

Section 2. The SEM images and XRD pattern of ZIF-8 membrane

Under the same ZIF-8 growth conditions and steps, we get purified ZIF-8 powder with good crystallized state and the particle size of about 126 nm as shown in Fig. S2a. As the SEM image in Fig. S2b shows, four cycles ZIF-8 has assembled on MNFs form a dense membrane with the thickness of 506.1 nm. Meanwhile, four growth cycles in situ self-assembled ZIF-8 membrane also have been grown on glass substrate at the same time with the MNFs*ZIF sensor, XRD pattern image consist with the standard powder diffraction files, and exhibits the good crystal structure of ZIF-8 membrane as demonstrated in Fig. S2c.

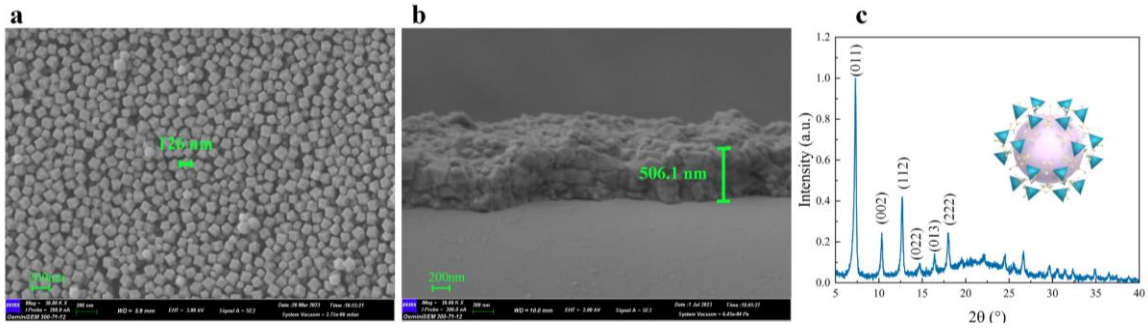

Fig. S2. a SEM image of purified ZIF-8 powders. **b** Cross sectional SEM image of ZIF-8 membrane. **c** The XRD patterns image of four cycle ZIF-8 on glass substrate.

Section 3. The reversibility and repeatability of the MNFs*ZIF

The proposed MNFs*ZIF can be continuously reused theoretically, and the sensor fabricated in the same batch is tested for the reversibility and repeatability. Due to limitations in experimental time and conditions, we tested it for 15 cycles, and the results demonstrated that the sensor could still work well with the integral process of evaporation, stabilization and exhaust, in which the mean Bland-Altman error is 6.92 nm within 6.46~7.39 nm. Without any performance degradation, it can be inferred that the sensor could be continuously reused according to the experimental results.

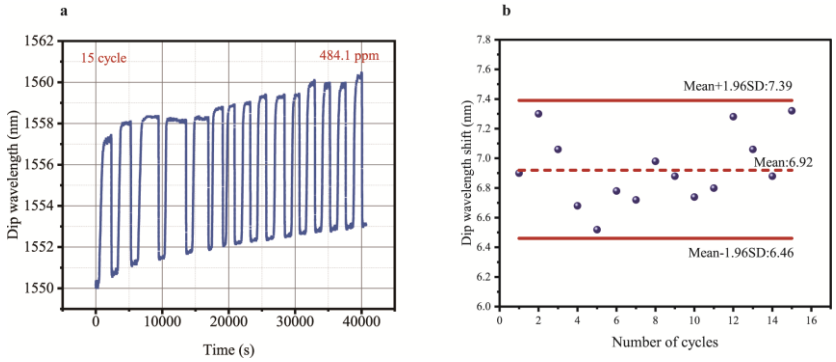

Fig. S3. The test of reused times **(a)** 15 cycles; **(b)** Bland-Altman error analysis of 15 cycles.

Section 4. Performance comparison of different VOCs optical fiber sensors

Table S1 presents the performance of different types VOCs sensors based on optical fiber in last decade, compared to these VOCs sensor, our MNFs*ZIF demonstrate an outstanding overall performance in terms of sensitivity, selectivity, response time and detection limitation.

Table S1. Optical fiber VOCs sensors performance in last decade

Principle	Sensitive layer	VOCs (Analyte status)	Dynamic range	Sensitivity	LOD	Responese time /Recovery time	Ref.	Selectivity
Long-period fiber grating	ZIF-8	Ethanol, Acetone (solution)	62-666 ppm, 49-543 ppm	0.018 nm/ppm 0.015 nm/ppm	5.56 ppm 6.67 ppm	10min/10min	1, 2	Y
Microfiber coupler	Nile red	Ethanol, Methanol (solution)	0-45 ppm, 0-65 ppm	-0.13 nm/ppm -0.036 nm/ppm	77 ppb 281 ppb	5min/8min	3	Y
Evanescent fiber	SnO_2	Ethanol (gas)	1000-20000 ppm	Nonlinear (10% at 5000 ppm)	-	10s/50s	4	N
Fiber tip SPR	Epoxy/Au /MoS_2	Methanol (gas)	-	− 0.0184 pm/ppm	-	-	5	Y
Photonic crystals fiber	Polystyrene nanospheres	Ethanol, Methanol et al VOCs (solution)	0-70%(v/v)	-	2%	-	6	Y
Microfiber	ZIF-8/GO	Methanol (solution)	343-6858 ppm	3.8 pm/ppm	5.26 ppm	118ms/-	7	Y
Microfiber	**ZIF-8**	**DMC (solution)**	**9.4-435.7 ppm**	**43.6 pm/ppm**	**2.65 ppm**	**10min/23s**	**This work**	**Y**

References

1. Hromadka, J., Tokay, B., Correia, R., Morgan, S.P. & Korposh, S. Highly sensitive volatile organic compounds vapour measurements using a long period grating optical fibre sensor coated with metal organic framework ZIF-8. Sens. Actuators, B **260**, 685-692 (2018).
2. Hromadka, J., Tokay, B., James, S., Tatam, R.P. & Korposh, S. Optical fibre long period grating gas sensor modified with metal organic framework thin films. Sens. Actuators, B **221**, 891-899 (2015).
3. Liu, D. et al. High sensitivity optical fiber sensors for simultaneous measurement of methanol and ethanol. Sens. Actuators, B **271**, 1-8 (2018).
4. Sharifpour-Boushehri, S., Hosseini-Golgoo, S.M. & Sheikhi, M-H. A low cost and reliable fiber optic ethanol sensor based on nano-sized SnO_2. Opt. Fiber Technol. **24**, 93-99 (2015).
5. Du, B. et al. MoS_2-enhanced epoxy-based plasmonic fiber-optic sensor for selective and sensitive detection of methanol. Sens. Actuators, B **305**, 127513 (2020).
6. Burratti, L. et al. Polystyrene photonic crystals as optical sensors for volatile organic compounds. Mater. Chem. Phys. **212**, 274-281 (2018).
7. Huang, Y. et al. Ultrafast response optical microfiber interferometric VOC sensor based on evanescent field interaction with ZIF-8/graphene oxide nanocoating. Adv. Opt. Mater. **10**, 2101561 (2022).